Evaluating the performance of two eddy-viscosity turbulence models to predict mixed convection in a rectangular room

Guilherme Anrain Lindner, guilherme@cardinal.com.br
Kátia Cordeiro Mendonça, k.mendonca@pucpr.br
Viviana Cocco Mariani, viviana.mariani@pucpr.br
Mechanical Engineering Department
Pontifical Catholic University of Paraná - PUCPR

Abstract. The goal of this work is to investigate the performance of two eddy viscosity turbulence models, standard k-ε and k-ω, in predicting the three-dimension airflow in a rectangular room whose floor is heated. The experimental data from Annex 20, which represents a large rectangular room where the air is supplied horizontally on the upper left and is exhausted through the opening on the lower right of the opposite side, were used to check the numerical results. The airflow is characterized by Reynolds and Archimedes numbers based on the height of the air inlet and on the difference of air temperature between the inlet and outlet openings, respectively. Air temperature and surface temperature profiles predicted by both turbulence models are compared to experimental results from current literature, considering high buoyancy effect (Re = 2,400 and Ar = 85×10^{-6}) and low buoyancy effect (Re = 7,100 and Ar =$1,1\times10^{-6}$). Additional results are presented in terms of mean velocity profiles and compared to experimental data for the isothermal case.

Keywords*: Computational Fluid Dynamics, mixed convection, indoor airflow, standard k-ε, k-ω, turbulence.*

1. INTRODUCTION

Airflows in enclosed environments involve one or all three types of convection: forced, natural or mixed convection. Accurate simulation of these flows is essential to improve and optimize ventilation systems and to save energy. In addition, different airflow patterns can lead to very different heat transfer coefficients and temperature distributions in confined spaces. The corresponding heat and loss will not be the same. The Computational Fluid Dynamic (CFD) simulations often use turbulence models, since most indoor flows are turbulent.

Forced and natural convection can be viewed as two extreme cases of mixed convection. Mixed convection is more complicated than forced convection and natural convection since it combines the effects of both (Xu and Chen, 2001). Turbulent forced convection has been extensively studied and most turbulence models are developed for forced flows. A review of the studies on turbulent natural convection can be found in (Xu *et al.*, 1998) and studies on turbulent forced convection can be seen in Nielsen (1990) and Nielsen *et al.* (1978). Zhai *et al.* (2007) summarized recent progress in CFD turbulence modeling and applications to some practical indoor environment studies.

Studies on turbulent mixed convection can be classified into three categories: theoretical analysis, experimental investigation and numerical simulation. Theoretical studies include those by Nakajima and Fukui (1980), Chen *et al.* (1987) and Aicher and Martin (1997). The notable contributions about experimental investigations on turbulent mixed convection are those by Schwenke (1975), Blay *et al.* (1992) and Nielsen (1990). The last study has been selected to validate the turbulence models applied in this paper.

Numerical simulations of mixed convection are available in literature. Nielsen *et al.* (1979) used the standard k-ε model with wall functions and calculated the flows in a ventilated room with a heated floor. The prediction agrees well with the experimental data, nevertheless it is known that the wall functions cannot calculate buoyancy effects accurately. Chen (1995) compared the performance of several k-ε models on indoor airflow simulation and found that the performance of RNG k-ε model is better in mixed convection than in forced convection flows. The RSM was applied by Chen (1996) on indoor airflow simulations, and the performance of this method is less satisfactory in mixed convection than in forced and natural convection. The model combining a near-wall one-equation model and a near-wall natural convection model with the aid of direct numerical simulation (DNS) was investigated by Xu and Chen (2001a), while the model using one-equation model for near-wall region and the standard k-ε model for the outer wall region was investigated by Xu and Chen (2001b) for predicting forced, natural and mixed convection.

The k-ω model has been recently used for a few indoor airflow and heat transfer simulations. Liu and Moser (2003) indicated that the shear stress transport (SST) k-ω model can predict the transient turbulent flow and heat transfer of forced ventilated fire in enclosures. Stamou and Katsiris (2006) used the SST k-ω model to predict air velocity and temperature distributions in a model office room. Kuznik *et al.* (2007) investigated the SST k-ω model with experimental measurements of air temperature and velocity for a mechanically ventilated room with a strong jet inflow. The k-ω model appears most reliable and can simulate the expansion rates in the highly anisotropic cold case at the same magnitude order as the measurements but not a match (Zhai *et al.*, 2007).

In summary, few studies have been developed for turbulent mixed convection due to its complexity. Most numerical simulations on the mixed convection have employed various versions of the group k-ε. Some others have applied the RSM, and only few studies have applied the k-ω model besides its undoubtedly potential for modeling indoor environment with good accuracy and numerical stability. Recently, one of the commercial CFD tools, CFX (ANSYS 2007), placed its emphasis on k-ω-equation-based turbulence models because of its multiple advantages, such as simple and robust formulation, accurate and robust wall treatment (low-Re formulation), high quality for heat transfer predictions, and easy combination with other models (Zhai *et al.*, 2007). Therefore, it is proposed in this work to evaluate the performance of the standard k-ε and k-ω models in order to contribute to reach a solid conclusion about modeling indoor airflows with heat transfer.

The remainder of the paper is organized as follows. In section 2, the governing equations are described. In section 3, it is presented the numerical methodology while in section 4 it is presented the case under investigation. Numerical results in terms of temperature and mean velocity profiles are compared to the available experimental data and are discussed in section 5. Lastly, section 6 summarizes the present work.

2. MODEL DESCRIPTION

Reynolds (1894) decomposed the Navier-Stokes equations in two parties, one related to the average value of the velocity vector and another related to its fluctuation, and applied the time average operator on them to study turbulent flows. The resulting set of equations is known as Reynolds Average Navier-Stokes (RANS) equations and gives information about the mean flow. Although this approach is not able to describe the multitude of length scales involved in turbulence, it has been largely used all of the word because in many engineering applications the information about the mean flow is quite satisfactory.

Considering that density and viscosity variations are small so that their effects on turbulence can be ignored, the fluid is Newtonian, the flow is incompressible and the steady state, the governing RANS equations in Cartesian coordinates can be expressed by (Versteeg and Malalasekera, 1995):

$$\frac{\partial U_i}{\partial x_i} = 0 , \tag{1}$$

$$\rho \frac{\partial (U_i U_j)}{\partial x_j} = -\frac{\partial P}{\partial x_i} + \frac{\partial}{\partial x_j}\left(\mu \frac{\partial U_i}{\partial x_j} - \rho \overline{u_i u_j} \right) + F_i , \tag{2}$$

where U_i and U_j are components of the average velocity vector [m/s], ρ is the fluid density [kg/m^3], μ is the dynamic viscosity of the fluid [Pa.s], P is the mean average pressure [Pa] and F_i is a component of the bulk force vector [N]. The extra-term that appears in Eq. (2) comparing to the original Navier-Stokes equations, $\overline{u_i u_j}$, is the product of fluctuation velocities [m^2/s^2] termed Reynolds stresses and is never negligible in any turbulent flow. It represents the increase in the diffusion of the mean flow due to the turbulence. Equations (1) and (2) can only be solved if the Reynolds stress tensor are known, a problem referred to as the 'closure problem' since the number of unknowns is greater than the number of equations.

The main goal of the turbulence studies based on RANS equations is therefore to determine the Reynolds stresses. According to Kolmogorov (1942) they can be evaluated by the following expression:

$$-\overline{u_i u_j} = \nu_t \left(\frac{\partial U_i}{\partial x_j} + \frac{\partial U_j}{\partial x_i} \right) - \frac{2}{3}\delta_{ij} k , \tag{3}$$

where δ_{ij} is the Kronecker delta and the kinetic energy of the turbulent motion, k, is defined as $k = \overline{u_i u_i}/2$ [m^2/s^2]. Substitution of Eq. (3) into Eq. (2) results in the average Navier-Stokes equations with the Reynolds stresses modeled via the viscosity concept,

$$\rho \frac{\partial (U_i U_j)}{\partial x_j} = -\frac{\partial P'}{\partial x_i} + \frac{\partial}{\partial x_j}\left[(\mu + \mu_t)\left(\frac{\partial U_i}{\partial x_j} + \frac{\partial U_j}{\partial x_i} \right) \right] + \rho\beta(T_0 - T) g_i \tag{4}$$

where μ_t is the turbulent viscosity, $P' = P + 2/3k$ is the modified pressure, β is the thermal expansion coefficient of air [1/K], T_0 is the temperature in a reference point [K], T is the temperature [K], and g is the gravity acceleration [m/s^2]. The last term on the right side of Eq. (4) takes into account of buoyancy effects.

The turbulent viscosity can be expressed as the product of a velocity scale, u [m/s], and a length scale, L_μ [m], $\mu_t = \rho u L_\mu$. Considering the velocity scale being calculated by $u = k^{1/2}$, Kolmogorov (1942) and Prandtl (1945) independently proposed the following relation for the turbulent viscosity,

$$\mu_t = \rho c_\mu k^{1/2} L_\mu , \tag{5}$$

where c_μ (=0.09) is an empiric constant.

The momentum equation, Eq. (4), is coupled to the energy equation by the buoyancy term, and also by thermodynamics properties and transport coefficients if they are temperature dependent. As a result, the conservation of energy, Eq. (6), must be solve to obtain both temperature and velocity fields,

$$\frac{\partial (U_j T)}{\partial x_j} = \frac{\partial}{\partial x_j}\left[\tau_{T,eff}\frac{\partial T}{\partial x_j}\right] + \dot{q}/\rho C_p \tag{6}$$

where $\tau_{T,eff}$ is effective turbulent diffusion coefficient for Temperature [m^2/s], $\dot{q}$ is the thermal source [W/m^3], and C_p is the specific heat at constant pressure [J/kgK].

In order to complete the set of equations described above, the most popular turbulence models define two other transport equations: one for the turbulent kinetic energy, k, and another for a variable that relates k to L_μ. These models are called two equations models, and two of them have been employed in this work: the standard k-ε model (Launder and Spalding, 1974) and the k-ω model (Wilcox, 1988).

Explicit formulations for the two turbulence models investigated, standard *k-ε and k-ω*, are described below.

2.2.1. k-ε model

Due to its robustness, economy and acceptable results for a considerable amount of flows the k-ε model has been the most used model for numerical predictions of industrial flows. However, it is known to have deficiencies in some situations involving streamline curvature, acceleration and separation. This model will be used because it is the turbulence model frequently used in the same computational domain adopted in this work

In this model, proposed by (Launder and Spalding, 1974), the second variable for the complementary transport equations is the rate of the viscous dissipation, ε [m^2/s^3], which is related to k by:

$$\varepsilon = k^{3/2} \big/ L \, . \tag{7}$$

Therefore, the set of equations concerning the standard k-ε model is composed of Eqs. (1), (4) ,(5), (6) and (7), and two transport equations for k and ε that are, respectively, given by:

$$\rho\frac{\partial (U_j k)}{\partial x_j} = \frac{\partial}{\partial x_j}\left[\left(\mu + \frac{\mu_t}{\sigma_k}\right)\frac{\partial k}{\partial x_j}\right] + \mu_t\left[\frac{\partial U_i}{\partial x_j} + \frac{\partial U_j}{\partial x_i}\right]\left[\frac{\partial U_i}{\partial x_j}\right] - \rho\varepsilon \tag{8}$$

$$\rho\frac{\partial (U_j \varepsilon)}{\partial x_j} = \frac{\partial}{\partial x_j}\left[\left(\mu + \frac{\mu_t}{\sigma_\varepsilon}\right)\frac{\partial \varepsilon}{\partial x_j}\right] + c_1\mu_t\frac{\varepsilon}{k}\left[\frac{\partial U_i}{\partial x_j} + \frac{\partial U_j}{\partial x_i}\right]\left[\frac{\partial U_i}{\partial x_j}\right] - c_2\rho\frac{\varepsilon^2}{k} \tag{9}$$

where c_1 = 1.42; c_2 = 1.92; σ_k = 1 e σ_ε = 1.22 are empirical constants.

As Eqs. (8) and (9) cannot describe correctly the movement of the fluid near solid surfaces, the so called wall-functions are required to make it applicable to the entire domain.

2.2.1. k-ω model

Kolmogorov (1942) proposed the first two-equation model of turbulence, which included one differential equation for k and a second for ω, defined as the rate of dissipation of energy per unit volume and time. Saffman (1970) independently formulated a similar two-equation k–ω model. The parameter ω can be considered “a frequency characteristic of the turbulence decay process” (Saffman, 1970) and is related to dissipation by

$$\omega = \frac{\varepsilon}{c_\mu^4 k} \, . \tag{10}$$

Wilcox and Alber (1972), Saffman and Wilcox (1974), and others cited in Wilcox (1998) have provided further improvements to the model. The version of the k–ω model presented by Wilcox (1988) is the one used here.

Wilcox (1988) proposed that the dissipation-rate equation of the k-ε model would be replaced by an equation for a specific dissipation rate defined as $\omega = k/\varepsilon$. This k-ω model predicts the behaviour of attached boundary layers in adverse pressure gradients more accurately than k-ε. models, but performs poorly in free shear flows (Bardina *et al.,* 1997). The vorticity, ω, is associated to the turbulent kinectic energy, k, by the following expression:

$$\mu_t = \rho \frac{k}{\omega}. \tag{11}$$

Thus, in the model proposed by Wilcox (1988) the transport equations for the turbulent kinetic energy k and the specific dissipation rate ω are defined by Eqs. (12) and (13), respectively,

$$\rho \frac{\partial (U_j k)}{\partial x_j} = \frac{\partial}{\partial x_j}\left[\left(\mu + \frac{\mu_t}{\sigma_k}\right)\frac{\partial k}{\partial x_j}\right] + \mu_t \left[\frac{\partial U_i}{\partial x_j} + \frac{\partial U_j}{\partial x_i}\right]\left[\frac{\partial U_i}{\partial x_j}\right] - \beta_1 \rho k \omega. \tag{12}$$

$$\rho \frac{\partial (U_j \omega)}{\partial x_j} = \frac{\partial}{\partial x_j}\left[\left(\mu + \frac{\mu_t}{\sigma_\omega}\right)\frac{\partial \omega}{\partial x_j}\right] + \alpha \mu_t \frac{\omega}{k}\left[\frac{\partial U_i}{\partial x_j} + \frac{\partial U_j}{\partial x_i}\right]\left[\frac{\partial U_i}{\partial x_j}\right] - \beta_2 \rho \omega^2, \tag{13}$$

where $\sigma_k = 2$, $\sigma_\omega = 2$, $\beta_1 = 0.09$, $\beta_2 = 0.075$ and $\alpha = 5/9$.

The main problem with the Wilcox model is its well known strong sensitivity to free stream values of ω. Depending on the value specified for ω at the inlet, a significant variation in the results of the model can be obtained. A possible solution to this deficiency is to use a combination of the k-ω model equations implemented near wall regions and the k-ε turbulence model to be employed in the bulk flow region.

3. NUMERICAL METHODOLOGY

The numerical solution of the governing equations was performed using the commercial computational fluid dynamics code CFX, version 11.0 (2007). In this code the conservation equations for mass, momentum, energy and turbulence quantities are solved using the finite volume discretization method generated by unstructured Voronoi Diagram. For this practice the solution domain is divided in small control volumes, using a non-staggered grid scheme, and the governing differential equations are integrated over each control volume with use the Gauss' theorem. The resulting discrete linear equations system is solved using an Algebraic Multigrid called Additive Correction accelerated Incomplete Lower Upper (ILU) factorization technique. It is an iterative solver whereby the exact solution of the equations is approached during the course of several iterations.

Three grid levels formed by 315,000, 400,000 and 500,000 volumes were used to simulate the investigated flow with each turbulence model. Each grid is denominated Case 1, Case 2, and Case 3, in this sequence, respectively. The refinement was mainly promoted in the entrance and walls of the environment, where flow property gradients are steeper. The convergence criteria was calculated using the normalized residual,

$$\tilde{r}_\phi = \frac{r_\phi}{a_p \Delta\phi} < \gamma, \tag{14}$$

where r_ϕ is the raw residual control volume imbalance, a_P is representative of the control volume coefficient, $\Delta\phi$ is a representative range of the variable in the domain, ϕ represent all variables and $\gamma = 10^{-5}$ is stopping criterion.

4. RESULTS AND DISCUSSIONS

4.1. Problem description

The measurements were carried out in a rectangular scaled-down room where the air enters horizontally at the top of one side and leaves the room at the bottom of the opposite side. Figure 1 shows a sketch of this experimental device, as well as the positions in which the temperature profiles were compared. In this work, the CFD simulations were conducted in the half of the full-scale geometry equivalent to the Annex 20 test cell with the following dimensions: height H = 3.0 m, length L = 3.0H, width W= 4.7H, inlet height h = 0.056H and outlet height t = 0.16H.

The inlet boundary conditions for the x direction, y direction and z direction velocity components were specified as $U = U_0$ and $V = W = 0$, respectively, with U_0 being the air average velocity in the inlet of the cavity obtained from Reynolds number based on the inlet height, $Re = U_0 h/\nu$, equals to 2,400 and 7,100. Regarding k, ε and ω, the inlet boundary conditions were calculated by $k_0 = 1.5(0.04U_0)^2$, $\varepsilon_0 = 10k^{3/2}/h$ and $\omega_0 = \varepsilon_0/0.09k_0$, respectively. Zero relative pressure and zero gradients for the other variables are applied as the boundary conditions for the outlet. At the solid boundaries the no-slip and the impermeable wall boundary conditions were imposed for the velocity components, that is, $U = V = W = 0$. The turbulence quanties k, ε and ω are nulls at the walls. With the exception of the floor, along which a constant heat flux was added, all walls were assumed adiabatic. Considering Arquimedes number based on temperature difference between supply and exhaust air, $Ar = \beta g h \Delta T / U_0^2$, of $Ar = 85 \times 10^{-6}$ and $Ar = 1.1 \times 10^{-6}$, the heat fluxes added to the floor are respectively 6.9×10^{-3} W/m^2 (Re = 2,400) and 2.3×10^{-3} W/m^2 (Re = 7,100), where ΔT is the temperature difference between supply and exhaust air.

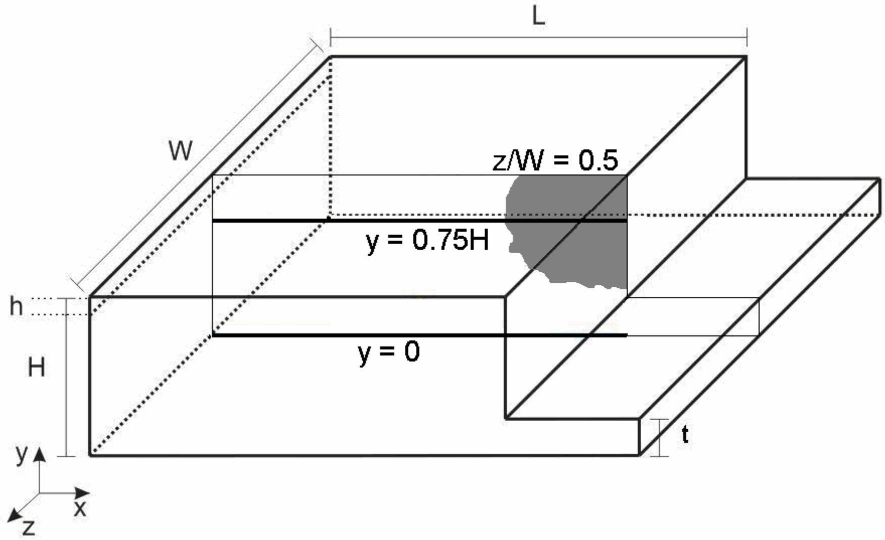

Figure 1. Flow geometry.

4.2. Result Analysis

Mixed convection is the most common flow encountered indoors, such as in summer when air conditioners are turned on. This section applies the two turbulence models, standard k-ε and k-ω to one validating case, concerning mixed convection in a ventilated room with a heated floor. Calculated and measured results are compared in Figs. 2 to 4. A grid-dependent study was conducted and the results are shown in Figs. 2 and 3. Fig. 2 compares the measured temperature at y/H = 0.75 and at y/H = 0, i.e., floor surface in the central plane of the room with the computational results predicted by the standard k-ε model (Figs. 2a and 2c) and by the k-ω model (Figs. 2b and 2d) that were obtained using three grid levels, for Re = 7,100 and $Ar = 1.1 \times 10^{-6}$.

For this case, with low buoyancy effect, the grid dependence analysis indicates that the calculation with 315,000 grid cells has already produced accurate results for the standard k-ε model (see Figs. 2a and 2c). Increasing the number of control volumes does not yield a better solution; in fact the results are worse. The non-coherent results obtained from more refined grids are attributed to the use of non-staggered grids. As the refinement was mainly promoted on the inlet and on the walls of the room, where the gradients are higher, this can be lead to less refined regions in order to adapted the numbers of grid cells to the entire domain. In this context a different behavior was observed for the k-ω model (see Figs. 2b and 2d). All three grids conducted to temperature profiles in accordance with experimental data for the air temperature at y/H = 0.75, however none of them was able to represent the surface temperature correctly, showing that a more important refinement might be necessary. This last comparison also indicates that the calculation with 500,000 grid cells produced slightly better results for k-ω turbulence model.

Results for Re = 2,400 and $Ar = 85 \times 10^{-6}$ are presented in Fig. 3. Figure 3 compares the computed profiles of temperature to the experimental data at y/H = 0.75 and y/H = 0 using the standard k-ε model (Figs. 3a and 3c) and the k-ω model (Figs. 3b and 3d). At y/H = 0.75 both turbulence models predict the air temperature adequately (see Figs. 3a and 3b). At the other position, y/H = 0, Fig. 3b indicates that the temperature profile predicted by the standard k-ε model is slightly lower than the measured profile but has the same shape. On the other hand, it can be seen in Fig. 3d that the k-ω model turbulence model greatly overpredicts the floor surface temperature. Again it can be inferred from these results that the k-ω model requires a more refined grid than the standard k-ε, although the commercial code also makes use of a wall-function for the k-ω model.

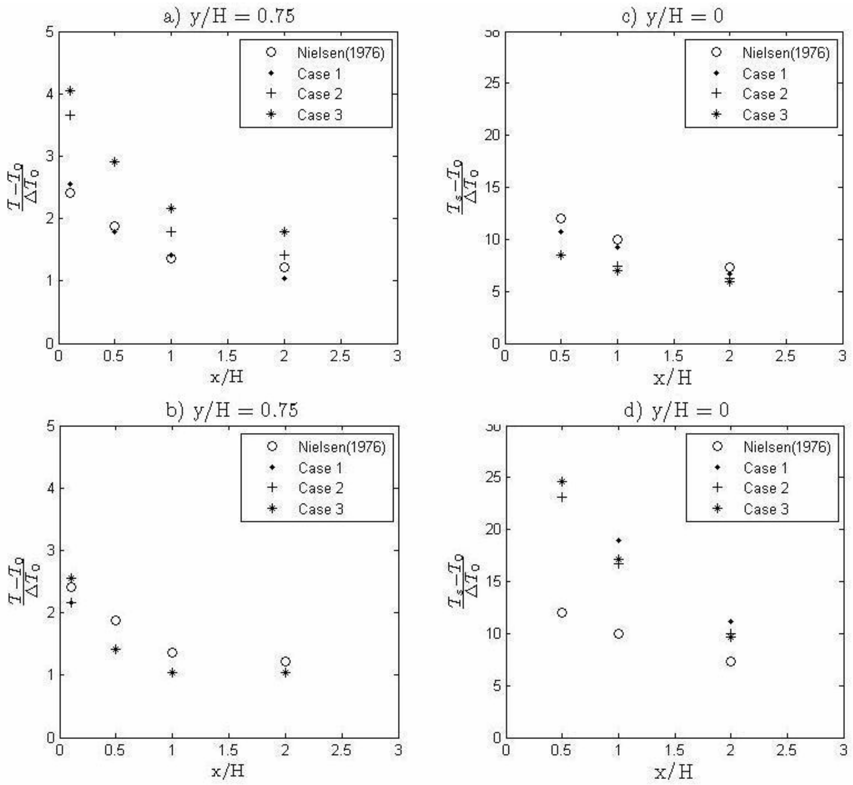

Figure 2. Grid-dependent study: temperature comparison between experimental data and predictions from the standard k-ε model (a, c) and k-ω model (b, d), for Re = 7,100 and Ar = 1.1×10^{-6}.

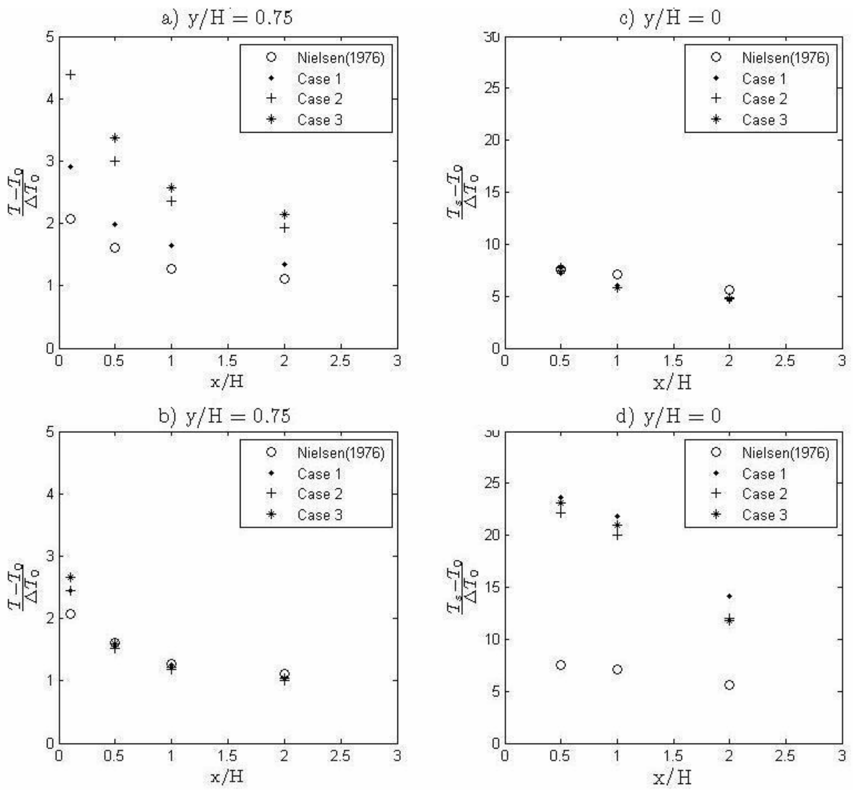

Figure 3. Grid-dependent study: temperature comparison between experimental data and predictions from the standard k-ε model (a, c) and k-ω model (b, d),, for Re = 2,400 and Ar = 85×10^{-6}.

The best numerical predictions for each turbulence model obtained from the grid-dependence study, with 315,000 grid cells for the standard k-ε model and with 500,000 for the k-ω model, are compared to each other and to the available experimental data in Fig. 4. Figures 4a and 4b illustrate that both computed air temperature profiles are in accordance to the experimental data, and the performance of the k-ω model is slightly better than that of the standard k-ε model for the case with high buoyancy effect. Nevertheless, as it has been observed before, the computed temperature profiles at the floor obtained from the k-ω model do not agree with the experimental data (see Figs. 4c and 4d), while the standard k-ε model reproduces quite well the temperature behavior of the floor. Therefore, these first results indicate that the performance of the standard k-ε model is better than that of k-ω model for both cases investigated.

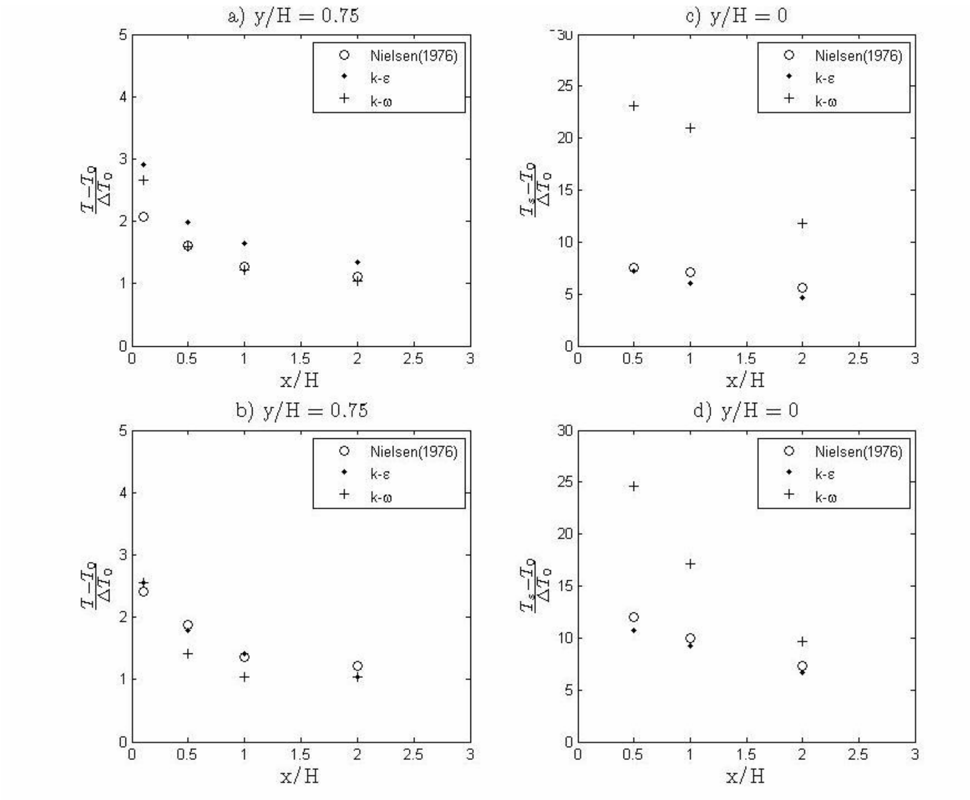

Figure 4. Turbulence model study: temperature comparison between predictions from both turbulence models investigated for Re = 7,100 and $Ar = 1.1\times10^{-6}$ (a, b) and Re = 2,400 and $Ar = 85\times10^{-6}$ (c, d).

In the following, the numerical results obtained from the two turbulence models investigated regarding the mean velocities at four positions of the central plane of the room, x = H, x = 2H, y = 0.028 H and y = 0.0972H, are compared to the experimental data from Nielsen (1990) for the isothermal case. The numerical results for Re = 7,100 and $Ar = 1.1\times10^{-6}$ are shown in Figure 5 while those for Re = 2,400 and $Ar = 85\times10^{-6}$ are shown in Figure 6. Analysing these figures, one can observe that, on the whole, the flow is described by the two turbulence models similarly. Both models have shown a reduction significant in the jet velocity (see Figs. 5.b and 5.d) specially in the case with higher bouyance effect (see Figs. 6a, 6b, and 6c), and a less intense recirculation on the right upper corner of the room (see Figs. 5d and 6d) mainly for k-ε model. An importante variation from the isothermal case is noted also in the lower part of the room, where the velocities are smaller, in both cases investigated (see Figs. 5c and 5d).

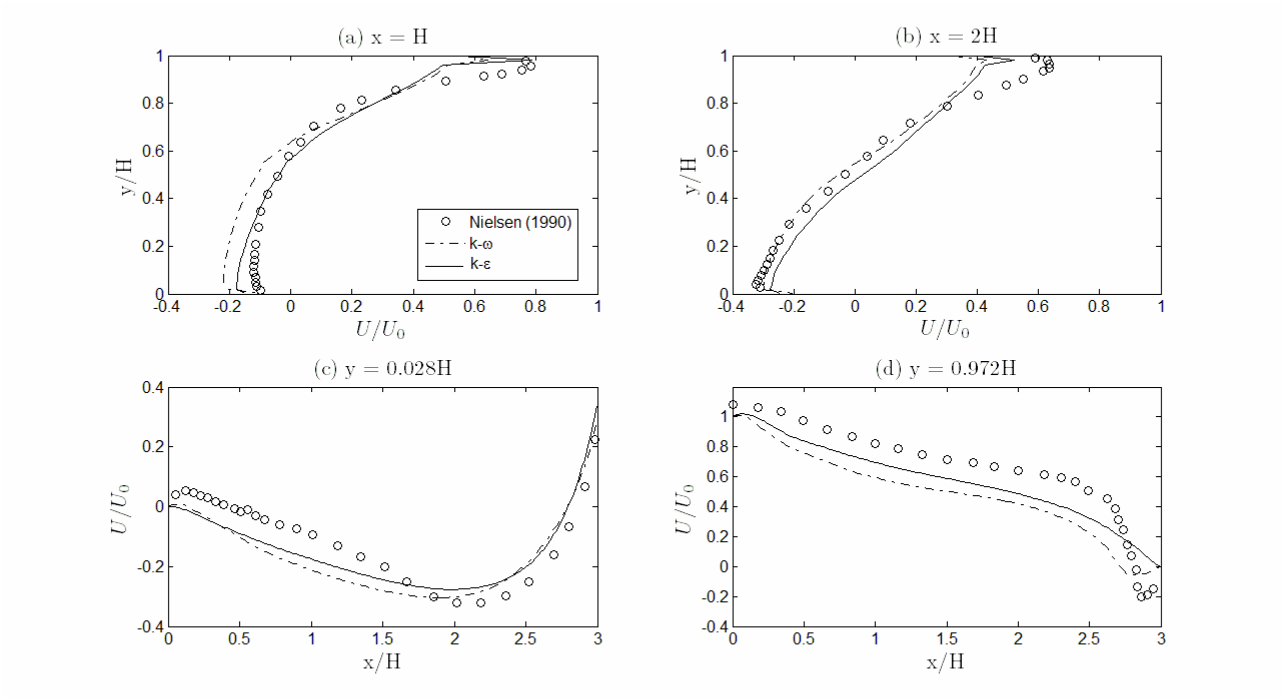

Figure 5. Turbulence model study: mean velocity comparison between experimental data for the isothermal case and predictions from both turbulence models investigated for *Re* = 7,100 and *Ar* = 1.1×10^{-6}.

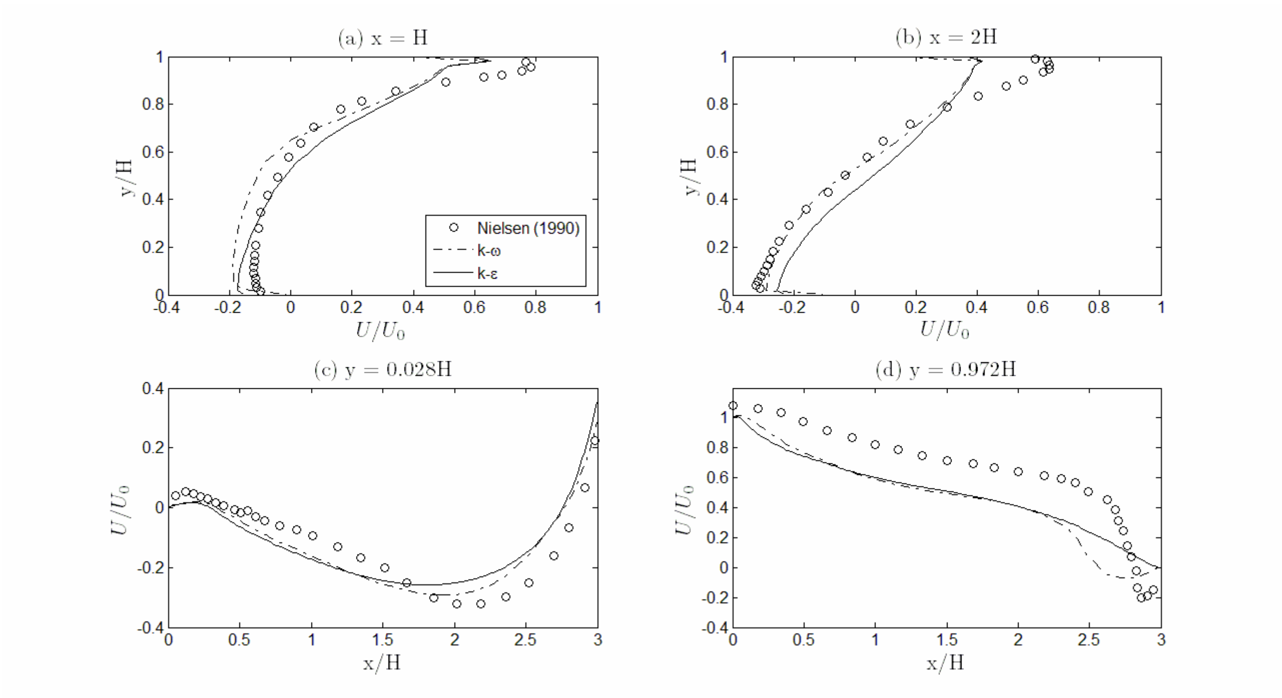

Figure 6. Turbulence model study: mean velocity comparison between experimental data for the isothermal case and predictions from both turbulence models investigated for *Re* = 2,400 and *Ar* = 85×10^{-6}.

5. CONCLUSIONS

The present work employed two eddy-viscosity turbulence models, standard *k*-ε and *k*-ω, to solve the airflow in a rectangular room under mixed convection. Numerical results regarding the air temperature and the floor surface temperature have been compared to the corresponding experimental data from Nielsen (1990), considering high and low buoyancy effects. In general, the performance of the standard k-ε model for such flows was better than that of the k-ω model. The k-ω model failed to predict temperature profiles at the floor, greatly overpredicting the temperature in that position. These first results confirm that the standard k-ε model has a good potential to simulate indoor airflow. However, further analysis must be carry out regarding the grid depence of both turbulence models for obtaining a more solid conclusion. Regarding the comparison of the behavior between the isothermal flow and the non-isothermal flow, the heat added to the floor seems to affect the jet core reducing its velocity, remembering that the preceding remarks about the grid dependence are also valid here.

6. REFERENCES

Aicher, T., Martin, H., 1997, New correlations for mixed turbulent natural and forced convection heat transfer in vertical tubes, International Journal of Heat Mass Transfer, Vol. 40, pp. 3617-3626.

Bardina, J. E., Huang, P. G. and Coakley, T. J., 1997, Turbulence modeling validation, testing, and development, *NASA-TM-110446*.

Blay, C., Mergui, S., Niculae, C., 1992, Confined turbulent mixed convection in the presence of a horizontal buoyant wall jet, Fundamentals of Mixed Convection, HTD 213, pp. 65-72.

Chen, Q., Comparison of different k-ε models for indoor air flow computations, Numerical Heat Transfer, Part B, Vol. 28, pp. 353-369.

Chen, Q., 1996, Prediction of room air motion by Reynolds-stress models, Building and Environment, Vol. 31, pp. 233-244.

Chen, T. S., Armaly, B. F., Ali, M. M., 1987, Turbulent mixed convection along a vertical plate, Journal of Heat Transfer, Vol. 109, pp. 251-253.

Kolmogorov, A.N., 1942, Equations of turbulent motion of an incompressible fluid. Izvestia Acad. Sci., USSR; Phys. Vol. 6, pp. 56–58.

Kuznik, F., Rusaouen, G., Brau, J., 2007, Experimental and numerical study of a full scale ventilated enclosure: Comparison of four two equations closure turbulence models, Building and Environment, Vol. 42, pp. 1043-1053.

Launder, B. E. and Spalding, D. B., 1974, The numerical computation of turbulent flows, Comp. Meth. Appl. Mech. Energy, Vol. 3, pp. 269-289.

Liu, Y., Moser, A., 2003, Numerical study of forced ventilated fire in enclosure. Proceedings of the 4th International Symposium on Heating, Ventilating and Air Conditioning, Beijing, China, pp. 243-250.

Menter, F. R., 1992, "Improved two-equation k-ω turbulence model for aerodynamic flows, NASA TM-103975, 1992.

Nakajima, M., Fukui, K., 1980, Buoyancy effects on turbulent transport in combined free and forced convection between vertical parallel plates, International Journal of Heat Mass Transfer, Vol. 23, pp. 1325-1336.

Nielsen, P. V., 1990, Specification of a two-dimensional test case, Technical report, International Energy Agency, Annex 20: Air Flow Pattern Within Buildings.

Nielsen, P. V., Restivo, A., Whitelaw, J. H., 1979, Buoyancy-affected flows in ventilated rooms, Numerical Heat Transfer, Vol. 2, pp. 115-127.

Nielsen, P. V., Restivo, A., Whitelaw, J. H., 1978, The velocity characteristics of ventilated rooms, Journal of Fluid Engineering, Vol. 100, pp. 291-298.

Prandtl, L., Wighardt, K., 1945, Über ein neues formelsystem für die ausgebildete turbulenz, Nachr. Akad. Wiss., Math.-Phys, Kl., 6.

Reynolds, O., 1895, On the dynamical theory of incompressible viscous fluids and the determination of the criterion, Phil. Trans. Roy. Soc. London A, Vol. 186, pp. 123-164.

Saffman, P.G., 1970, A model for inhomogeneous turbulent flow. Proc. R. Soc., London A, Vol. 317, pp. 417–433.

Saffman, P.G. and Wilcox, D.C., 1974, Turbulence-model predictions for turbulent boundary layers. AIAA Journal, Vol. 12, pp. 541–546.

Schwenke, H., 1975, Ueber das Verhalten elener horizontaler Zuluftstrahlen im begrenzten Raum, Luft-und Kaltetechnik, Vol. 5, pp. 241-246.

Stamou, A., Katsiris, I., 2006, Verification of a CFD model for indoor airflow and heat transfer. Building and Environment, Vol. 41, pp. 2171-2181.

Versteeg, H. K. and Malalasekera, W., 1995, An introduction to computational fluid dynamics, Longman Scientific & Technical, New York.

Wilcox, D.C. and Alber, I.E., 1972, A turbulence model for high speed flows. In: Proc. of the 1972 Heat Trans. & Fluid Mech. Inst.. Stanford Univ. Press, Stanford, CA, pp. 231–252.

Wilcox, D.C., 1988, Reassessment of the scale determining equation for advance turbulence models. AIAA Journal, Vol. 26, pp. 1299–1310.

Wilcox, D.C., 1998, Turbulence modeling for CFD. DCW Industries, Inc, La Canada, CA. p. 540

Xu, W., Chen, Q., 2001a, A two-layer turbulence model for simulating indoor airflow, Part I. Model development, Energy and Buildings, Vol. 33, pp. 613-625.

Xu, W., Chen, Q., 2001b, A two-layer turbulence model for simulating indoor airflow, Part I. Applications, Energy and Buildings, Vol. 33, pp. 627-639.

Xu, W., Chen, Q., Nieuwstadt, F. T. M., 1998, A new turbulence model for near-wall natural convection, International Journal of Heat Mass Transfer, Vol. 41, pp. 3161-3176.

Zhai Z, Zhang Z, Zhang, W, Chen, Q., 2007, Evaluation of various turbulence models in predicting airflow and turbulence in enclosed environments by CFD: Part-1: summary of prevalent turbulence models. HVAC&R Research, Vol. 13, pp. 1-21.

7. RESPONSIBILITY NOTICE

The authors Guilherme Anrain Lindner, Kátia Cordeiro Mendonça and Viviana Cocco Mariani are the only responsible for the printed material included in this paper.